Particle production in high-energy collisions beyond the shockwave limit

Tolga Altinoluk[a] and Adrian Dumitru[b,c]
[a] *Departamento de Física de Partículas and IGFAE, Universidade de Santiago de Compostela, E-15706 Santiago de Compostela, Galicia-Spain*
[b] *Department of Natural Sciences, Baruch College, CUNY, 17 Lexington Avenue, New York, NY 10010, USA*
[c] *The Graduate School and University Center, The City University of New York, 365 Fifth Avenue, New York, NY 10016, USA*

We compute next to eikonal (NE) and next to next to eikonal (NNE) corrections to the Lipatov vertex due to a finite target thickness. These arise from electric field insertions into the eikonal Wilson lines. We then derive a k_T-factorization formula for single inclusive gluon production at NNE accuracy and find that nuclear effects are absent. We also analyze NNE corrections to two-gluon production where some of the contributions are found to exhibit corrections proportional to $A^{2/3}$.

arXiv:1512.00279v3 [hep-ph] 24 Oct 2016

Production of particles with moderately high transverse momentum in high-energy hadronic collisions probes the gluon fields of the projectile or target at small light-cone momentum fractions [1]. The field (in light-cone gauge, $A^+ = 0$) in the forward light cone of a collision of two infinitely thin charge sheets (shock waves) is given by [2–4]

$$p^2 A^{i,a}(p) = (T^a)_{bc}\, g^3 \int dz_1^- dz_2^+ \int \frac{d^2k}{(2\pi)^2} L^i(p,k)\, \frac{\rho_1^b(z_1^-,k)\, \rho_2^c(z_2^+,p-k)}{k^2\,(p-k)^2}\ . \tag{1}$$

Here p is the transverse momentum of the produced gluon and $L^i(p,k)$ is the Lipatov vertex [5],

$$L_i(p,k)\, L_i^*(p,q) = \frac{4}{p^2}\left[\delta^{ij}\delta^{lm} + \epsilon^{ij}\epsilon^{lm}\right]\, k^i(p-k)^j\, q^l(p-q)^m\ . \tag{2}$$

In eq. (1) $\rho_{1,2}$ denote the random color charge densities of projectile and target, respectively, which will be averaged over. The equation is valid to leading order in both color charge densities; a generalization to all orders in ρ_2 was given in ref. [6].

Eq. (2) applies in the shockwave limit where the projectile charges propagate on eikonal trajectories through the field generated coherently by all valence charges in the target. Ref. [4], for example, offers a very clear discussion. However, at finite energies the non-zero thickness ℓ^+ of the target should be taken into account when $p^2\,\ell^+/p^+ \sim p\,\ell^+ e^{-y}$ is not negligible. This is the case, in particular, for heavy-ion targets since $\ell^+ \sim A^{1/3}$. We should emphasize that our focus here is not on finite-x corrections to the small-x evolution of the unintegrated gluon distribution. Such evolution equations for some specific gluon distributions have been derived in ref. [7] to order $(\ell^+/p^+)^0$. Furthermore, kinematic finite energy corrections not proportional to the target thickness have been derived by Babansky and Balitsky [8]; they find that such corrections are important for dipole-dipole scattering at rapidity $\lesssim 5$. Rather, here we consider corrections to the particle production vertex beyond the shockwave approximation for the *valence* charges; this is a nuclear effect proportional to $A^{1/3}$ and should be relevant in particular for a heavy-ion target.

The gluon production cross section then involves one or more electric field insertions into the eikonal Wilson lines [9, 10], i.e. operators such as

$$\mathcal{U}^{i,ab}_{[0,1]}(x^+,y^+,y_\perp) = \int_{y^+}^{x^+} dz^+ \frac{z^+-y^+}{x^+-y^+}\, \mathcal{U}^{ac}(x^+,z^+,y_\perp)\, \left[ig T^e_{cd}\partial_{y^i} A^{-,e}(z^+,y_\perp)\right]\, \mathcal{U}^{db}(z^+,y^+,y_\perp)\ , \tag{3}$$

where

$$\mathcal{U}(x^+,y^+,y_\perp) = \mathcal{P}\, e^{\,ig\int_{y^+}^{x^+} dz^+ T\cdot A^-(z^+,y_\perp)} \tag{4}$$

are the usual eikonal lines. Note that besides the electric field insertion which is due to the finite target thickness the Wilson line (3) does run along the light cone. For a study of kinematic corrections corresponding to Wilson lines at a finite angle (rapidity) we refer to ref. [8].

The new Wilson lines with electric field insertions appear due to quantum diffusion of the incident projectile in the transverse direction as it passes through a target of finite thickness. At leading order in the field of the target the

above Wilson line simplifies to

$$\mathcal{U}^{i,ab}_{[0,1]}(x^+,y^+,y_\perp) = \int\limits_{y^+}^{x^+} dz^+ \frac{z^+-y^+}{x^+-y^+}\,\left[igT^e_{ab}\partial_{y^i}A^{-,e}(z^+,y_\perp)\right] \tag{5}$$

which suffices for the evaluation of the Lipatov vertex. The purpose of this paper is to derive L_i at next to next to eikonal (NNE) accuracy; and to discuss the corrections to the single-inclusive gluon production cross section at high transverse momentum at order $\rho_T(k_1)\,\rho^*_T(k_2)$.

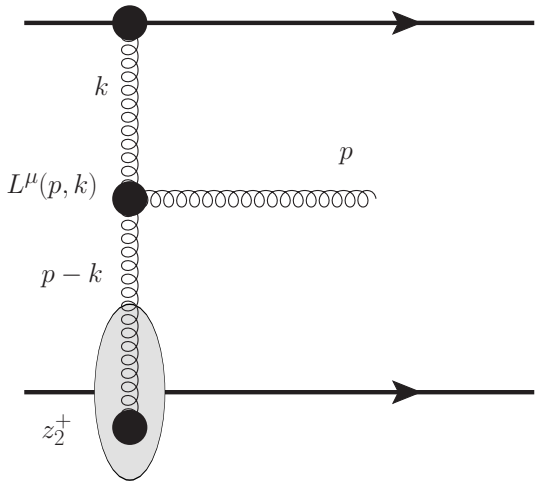

FIG. 1: Fusion of the fields of two high-energy projectile and target charges described by the Lipatov vertex.

Our result for the Lipatov vertex (in light-cone gauge $A^+=0$) at NNE accuracy is

$$L^i(p,k) = -2C^i(p,k)\;k^2\left\{1+\frac{i}{2}p^2\frac{z_2^+}{p^+}-\frac{1}{8}\left(p^2\frac{z_2^+}{p^+}\right)^2\right\}\;, \tag{6}$$

where

$$C^i(p,k) = \frac{p^i}{p^2}-\frac{k^i}{k^2}\;. \tag{7}$$

A derivation is given in appendix A and the corresponding diagram is shown in fig. 1. The first term in (6) corresponds to the eikonal (shock wave) limit while the second and third terms are the NE and NNE corrections for a target of finite thickness ℓ^+, respectively. These corrections come with additional factors of z_2^+/p^+ which is due to the above mentioned quantum diffusion of the incident wave passing through the target. The mean square deviation from the classical (eikonal) path is proportional to z_2^+/p^+ [10].

The vertex from eq. (6) acts on a product of projectile and target fields to generate the produced gluon radiation field in the forward light cone,

$$\mathcal{M}^a_\lambda(p) = \epsilon^i_\lambda\, p^2 A^{i,a}(p)\;, \tag{8}$$

with $p^2A^{i,a}(p)$ as written in eq. (1) above.

To compute the single inclusive cross section we multiply eq. (8) with its complex conjugate, sum over gluon polarizations and colors, and perform an average over the random color charge densities of projectile and target. In the standard McLerran-Venugopalan (MV) model [11] this (target) average is performed with the action

$$S_{\rm MV}[\rho] = \int d^2x_\perp \int\limits_0^{\ell^+} dx^+\;\frac{\mathrm{tr}\,\rho(x^+,x_\perp)\rho(x^+,x_\perp)}{\mu^2}\;, \tag{9}$$

which leads to the following color charge correlator:

$$\left\langle \rho^a(z_1^+,k_1)\,\rho^{*b}(z_2^+,k_2)\right\rangle = \delta^{ab}\,\delta(z_1^+-z_2^+)\,(2\pi)^2\delta^2(k_1-k_2)\,\mu^2\;. \tag{10}$$

μ^2 denotes the mean color charge density (squared) per unit transverse area and longitudinal phase space. Because color charge correlations in the MV model are local in z^+, sub-eikonal corrections, i.e. the curly brackets in eq. (6), cancel[14] in the (absolute) square of the amplitude (8).

One may also consider a generalization of the MV-model action where the two color charge densities sit at different longitudinal coordinates,

$$S_{\rm eff}[\rho] = \int d^2x_\perp \int_0^{\ell^+} dx^+ \int_{x^+-\lambda^+}^{x^++\lambda^+} \frac{dy^+}{2\lambda^+} \frac{{\rm tr}\,\rho(x^+,x_\perp)U_{x^+\to y^+}\rho(y^+,x_\perp)U_{y^+\to x^+}}{\mu^2} \ , \tag{11}$$

and are connected by gauge links along the longitudinal axis. λ^+ denotes the color correlation length in the target which should be on the order of the size of a nucleon.

At leading order in gA^- we then consider the color charge correlator

$$\left\langle \rho^a(z_1^+,k_1)\,\rho^{*b}(z_2^+,k_2)\right\rangle = \delta^{ab}\,\Theta(\lambda^+-|z_1^+-z_2^+|)\frac{1}{2\lambda^+}\,(2\pi)^2\delta^2(k_1-k_2)\,\mu^2 \ . \tag{12}$$

This correlator reduces to the MV-model one from eq. (10) in the limit $\lambda^+\to 0$.

In appendix B we show that eq. (12) leads to the single-inclusive cross section

$$p^+\frac{d\sigma}{dp^+d^2p\,d^2b} \ = \ 4N_c(N_c^2-1)\,S_\perp\frac{g^2}{p^2}\left[1-\frac{1}{6}\left(\frac{p^2\,\lambda^+}{2p^+}\right)^2\right]\int\frac{d^2k}{(2\pi)^2}\,\Phi_P(k^2)\,\Phi_T((p-k)^2) \ . \tag{13}$$

Here, $S_\perp$ denotes the transverse area of the collision. In eq. (13) we introduced the unintegrated gluon distribution of the target via

$$\Phi_T(k^2) = g^2\ell^+\,\frac{\mu_T^2}{k^2} \ , \tag{14}$$

and similar for the projectile. This function is dimensionless and proportional to the saturation momentum squared, $Q_s^2\sim g^4\ell^+\mu^2$. However, saturation of the gluon density at low k^2 is not incorporated in (14) which exhibits the perturbative $\sim 1/k^2$ growth down to low transverse momentum.

We note that in eq. (13) NE corrections $\sim p^2\lambda^+/p^+$ drop out, see also refs. [9, 10] and appendix B. The NNE correction corresponds to the second term in the square brackets. As already indicated above it is suppressed by two powers of the light-cone momentum p^+ of the produced gluon but increases with transverse momentum. Nevertheless, the NNE correction to single-inclusive gluon production is seen not to exhibit nuclear enhancement since it involves the color correlation scale λ^+ rather than the target thickness ℓ^+. This occurs because the gluon field of the target is evaluated at a longitudinal coordinate z_2^+ in the amplitude, and $\bar z_2^+$ in the conjugate amplitude which may differ at most by λ^+.

Next, we consider two gluon inclusive production. A detailed derivation is provided in appendix C. Here, we only summarize the main results.

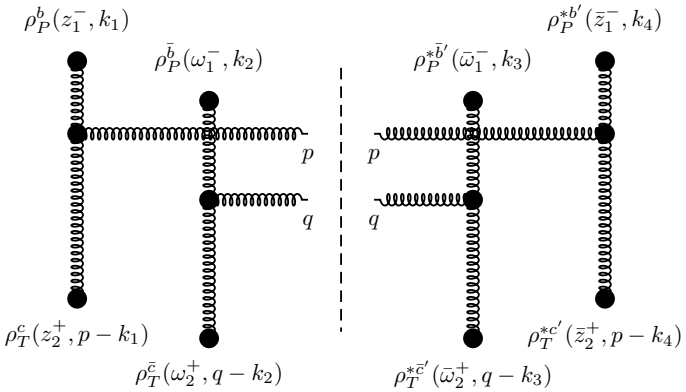

FIG. 2: Double inclusive gluon production

In the linear approximation two gluon production corresponds to the diagram shown in fig. 2 which has to be summed over all possible contractions of the sources in the projectile and target, respectively [12]. Just as in the

above we assume that the projectile can be approximated by an infinitely thin shock wave but we allow for a finite thickness $\ell^+ \sim A^{1/3}$ of the target. For simplicity, we restrict the discussion here to the local (in z^+) model, eqs. (9,10). In this case, sub-eikonal corrections cancel when one performs a contraction of the same sources in the amplitude and in its complex conjugate (denoted as "type A" diagrams in appendix C). On the other hand, NNE corrections do not cancel when ρ_1 is contracted with ρ_2^* and ρ_1^* is contracted with ρ_2 ("type B" diagrams in appendix C), or when ρ_1 is contracted with ρ_2 and ρ_1^* with ρ_2^* ("type C" diagrams in appendix C). These diagrams again involve a correction of order

$$\left(\frac{\ell^+ p^2}{p^+}\right)^2 \tag{15}$$

which is proportional to $A^{2/3}$. The full result for the inclusive two gluon production cross section is

$$\begin{aligned}
p^+q^+\frac{d\sigma}{dp^+d^2pdq^+d^2q} &= 16N_c^2(N_c^2-1)\,g^4\frac{S_\perp}{p^2q^2}\int\frac{d^2k_1}{(2\pi)^2}\frac{d^2k_2}{(2\pi)^2}\Phi_P(k_1^2)\Phi_P(k_2^2)\Phi_T\left[(p-k_1)^2\right]\Phi_T\left[(q-k_2)^2\right] \\
&\quad\Big[\delta^{(2)}(k_1+k_2)+\delta^{(2)}(k_1-k_2) \\
&+\frac{1}{8}\delta^{(2)}(p-q-k_1+k_2)\left[1-\frac{1}{12}\left(\frac{p^2}{2p^+}-\frac{q^2}{2q^+}\right)^2\ell^{+2}\right] \\
&\quad\times\left\{1+\frac{k_2^2(p-k_1)^2}{k_1^2(p+k_2)^2}-\frac{p^2(k_1+k_2)^2}{k_1^2(p+k_2)^2}\right\}\left\{1+\frac{k_1^2(q-k_2)^2}{k_2^2(q+k_1)^2}-\frac{q^2(k_1+k_2)^2}{k_2^2(q+k_1)^2}\right\} \\
&+\frac{1}{4}\delta^{(2)}(p-q)\left[1-\frac{1}{12}\left(\frac{p^2}{2p^+}-\frac{q^2}{2q^+}\right)^2\ell^{+2}\right] \\
&\quad\times\left\{1+\frac{k_2^2(p-k_1)^2}{k_1^2(p-k_2)^2}-\frac{p^2(k_1-k_2)^2}{k_1^2(p-k_2)^2}\right\}\left\{1+\frac{k_1^2(q-k_2)^2}{k_2^2(q-k_1)^2}-\frac{q^2(k_1-k_2)^2}{k_2^2(q-k_1)^2}\right\} \\
&+\delta^{(2)}(p-q-k_1+k_2)\left[1-\frac{1}{12}\left(\frac{p^2}{2p^+}-\frac{q^2}{2q^+}\right)^2\ell^{+2}\right] \\
&+\frac{1}{4}\delta^{(2)}(p+q)\left[1-\frac{1}{12}\left(\frac{p^2}{2p^+}+\frac{q^2}{2q^+}\right)^2\ell^{+2}\right] \\
&\quad\times\left\{1+\frac{k_2^2(p-k_1)^2}{k_1^2(p+k_2)^2}-\frac{p^2(k_1+k_2)^2}{k_1^2(p+k_2)^2}\right\}\left\{1+\frac{k_1^2(q-k_2)^2}{k_2^2(q+k_1)^2}-\frac{q^2(k_1+k_2)^2}{k_2^2(q+k_1)^2}\right\} \\
&+\frac{1}{8}\delta^{(2)}(p+q-k_1-k_2)\left[1-\frac{1}{12}\left(\frac{p^2}{2p^+}+\frac{q^2}{2q^+}\right)^2\ell^{+2}\right] \\
&\quad\times\left\{1+\frac{k_2^2(p-k_1)^2}{k_1^2(p-k_2)^2}-\frac{p^2(k_1-k_2)^2}{k_1^2(p-k_2)^2}\right\}\left\{1+\frac{k_1^2(q-k_2)^2}{k_2^2(q-k_1)^2}-\frac{q^2(k_1-k_2)^2}{k_2^2(q-k_1)^2}\right\} \\
&+\delta^{(2)}(p+q-k_1-k_2)\left[1-\frac{1}{12}\left(\frac{p^2}{2p^+}+\frac{q^2}{2q^+}\right)^2\ell^{+2}\right] \\
&\quad\Big]\,.
\end{aligned} \tag{16}$$

This expression does not include the disconnected contribution corresponding to uncorrelated production of the two gluons. The fact that NNE corrections do appear in the two-gluon cross section and that they are not the same for all diagrams could be important for studies of two-particle azimuthal correlations. However, more detailed computations with realistic unintegrated gluon densities, and including the dijet contribution are required [13] for more quantitative statements.

In summary, in this paper we have evaluated explicitly Wilson lines with electric field insertions to leading order in the field gA^- of the target. This determines next to eikonal (NE) and next to next to eikonal (NNE) corrections to the Lipatov vertex which are proportional to powers of the target thickness, and hence to $A^{1/3}$. From the vertex we have derived a k_T-factorization formula valid up to NNE accuracy. For single inclusive gluon production we find that sub-eikonal corrections cancel if a model with local (in the longitudinal coordinate z^+) color charge correlator for the target is employed. On the other hand such corrections should be present in models with color charge correlators with finite support. Furthermore, NNE eikonal corrections also appear in correlated two gluon production, even for a local

target color charge correlator. Rather than simply rescaling the two-gluon cross section we find that NNE corrections depend on the type of contractions of the sources in the target. Thus, such corrections may affect two-particle angular correlations when $\ell^+ p^2/p^+$ is not very small.

Acknowledgments

T.A. expresses his gratitude to the Department of Natural Sciences of Baruch College for their warm hospitality during a visit when this work was done. T.A. acknowledges support by the People Programme (Marie Curie Actions) of the European Union's Seventh Framework Programme FP7/2007-2013/ under REA grant agreement #318921; the European Research Council grant HotLHC ERC-2011-StG-279579, Ministerio de Ciencia e Innovación of Spain under project FPA2014-58293-C2-1-P, Xunta de Galicia (Consellería de Educación and Consellería de Innovación e Industria - Programa Incite), the Spanish Consolider-Ingenio 2010 Programme CPAN and FEDER. A.D. gratefully acknowledges support by the DOE Office of Nuclear Physics through Grant No. DE-FG02-09ER41620; and from The City University of New York through the PSC-CUNY Research grants 67119-0045 and 69362-0047.

Appendix A: The Lipatov vertex to NNE level

In this appendix we provide details of the calculation of NE and NNE corrections to the Lipatov vertex. The gluon-nucleus reduced amplitude[15] at NNE accuracy [10] is given by

$$\begin{aligned}\overline{M}^{ab}_{\lambda}(\underline{p},k) = i\varepsilon^{*i}_{\lambda}\int d^2x\, e^{ix\cdot(k-p)}\Bigg\{&2C^i(p,k)\,\mathcal{U}(\ell^+,0;x) + \frac{\ell^+}{p^+}\left[\left(\delta^{ij}-2p^j\frac{k^i}{k^2}\right)\mathcal{U}^j_{[0,1]}(\ell^+,0;x) - i\frac{k^i}{k^2}\mathcal{U}_{[1,0]}(\ell^+,0;x)\right]\\ &+\left(\frac{\ell^+}{p^+}\right)^2\left[-\frac{k^i}{k^2}p^jp^l\mathcal{U}^{jl}_{[0,2]}(\ell^+,0;x) - i\frac{k^i}{k^2}p^j\mathcal{U}^j_{[1,1]}(\ell^+,0;x) + \frac{1}{2}\frac{k^i}{k^2}\mathcal{U}_{[2,0]}(\ell^+,0;x)\right.\\ &\left.+\frac{i}{4}\left(p^2\delta^{ij}-2p^ip^j\right)\mathcal{U}^j_{(\mathrm{A})}(\ell^+,0;x) + \frac{1}{4}p^j\mathcal{U}^{ij}_{(\mathrm{B})}(\ell^+,0;x) + \frac{i}{4}\mathcal{U}^i_{(\mathrm{C})}(\ell^+,0;x)\right]\Bigg\}, \end{aligned} \tag{A1}$$

where $(\underline{p}) \equiv (p^+,p)$[16]. This expression is valid to all orders in the field of the target. To compute the Lipatov vertex we expand the standard or decorated Wilson lines to linear order in the charge density of the target, $g\rho_T$. For the standard Wilson line,

$$\int d^2x\, e^{ix\cdot(k-p)}\mathcal{U}(\ell^+,0;x)^{ab} = (2\pi)^2\delta(k-p)1^{ab} + i\,g^2T_c^{ab}\frac{1}{(p-k)^2}\int_0^{\ell^+}dz^+\rho_T^c(z^+,p-k) + O(\rho_T^2). \tag{A2}$$

The decorated Wilson lines that appear at NE and NNE level are Wilson lines with one or more background field insertions along the longitudinal axis from 0 to ℓ^+. For the explicit expressions of these decorated Wilson lines, we refer to ref. [10]. The expansion of each field insertion starts at linear order in ρ_T. Thus, terms with multiple field insertions contribute at higher orders in ρ_T and can be neglected at linear order. Keeping this in mind, we obtain the following expressions for the decorated Wilson lines:

$$\int d^2x\, e^{ix\cdot(k-p)}\mathcal{U}^j_{[0,1]}(\ell^+,0,x)^{ab} = -g^2T_c^{ab}\frac{(p-k)^j}{(p-k)^2}\int_0^{\ell^+}dz^+\left(\frac{z^+}{\ell^+}\right)\rho_T^c(z^+,p-k) + O(\rho_T^2) \tag{A3}$$

$$\int d^2x\, e^{ix\cdot(k-p)}\mathcal{U}_{[1,0]}(\ell^+,0,x)^{ab} = -ig^2T_c^{ab}\int_0^{\ell^+}dz^+\left(\frac{z^+}{\ell^+}\right)\rho_T^c(z^+,p-k) + O(\rho_T^2) \tag{A4}$$

$$\int d^2x\, e^{ix\cdot(k-p)}\mathcal{U}^{jl}_{[0,2]}(\ell^+,0,x)^{ab} = -ig^2T_c^{ab}\frac{(p-k)^j(p-k)^l}{(p-k)^2}\int_0^{\ell^+}dz^+\left(\frac{z^+}{\ell^+}\right)^2\rho_T^c(z^+,p-k) + O(\rho_T^2) \tag{A5}$$

$$\int d^2x\, e^{ix\cdot(k-p)}\mathcal{U}^j_{[1,1]}(\ell^+,0,x)^{ab} = g^2T_c^{ab}(p-k)^j\int_0^{\ell^+}dz^+\left(\frac{z^+}{\ell^+}\right)^2\rho_T^c(z^+,p-k)+O(\rho_T^2) \tag{A6}$$

$$\int d^2x\, e^{ix\cdot(k-p)}\mathcal{U}_{[2,0]}(\ell^+,0,x)^{ab} = ig^2T_c^{ab}(p-k)^2\frac{1}{2}\int_0^{\ell^+}dz^+\left(\frac{z^+}{\ell^+}\right)^2\rho_T^c(z^+,p-k)+O(\rho_T^2) \tag{A7}$$

$$\int d^2x\, e^{ix\cdot(k-p)}\mathcal{U}^j_{(\mathrm{A})}(\ell^+,0,x)^{ab} = -g^2T_c^{ab}\frac{(p-k)^j}{(p-k)^2}\int_0^{\ell^+}dz^+\left(\frac{z^+}{\ell^+}\right)^2\rho_T^c(z^+,p-k)+O(\rho_T^2) \tag{A8}$$

$$\int d^2x\, e^{ix\cdot(k-p)}\mathcal{U}^{ij}_{(\mathrm{B})}(\ell^+,0,x)^{ab} = -ig^2T_c^{ab}[\delta^{ij}\delta^{lm}+\delta^{il}\delta^{jm}+\delta^{im}\delta^{jl}]\frac{(p-k)^l(p-k)^m}{(p-k)^2} \times\int_0^{\ell^+}dz^+\left(\frac{z^+}{\ell^+}\right)^2\rho_T^c(z^+,p-k)+O(\rho_T^2) \tag{A9}$$

$$\int d^2x\, e^{ix\cdot(k-p)}\mathcal{U}^i_{(\mathrm{C})}(\ell^+,0,x)^{ab} = g^2T_c^{ab}(p-k)^i\int_0^{\ell^+}dz^+\left(\frac{z^+}{\ell^+}\right)^2\rho_T^c(z^+,p-k)+O(\rho_T^2) \tag{A10}$$

Using the expressions above, it is straightforward to obtain the amplitude at order ρ_T as

$$\overline{M}^{ab}_\lambda(\underline{p},k) = i\varepsilon^{*i}_\lambda(ig^2)T_c^{ab}\frac{1}{(p-k)^2}\int_0^{\ell^+}dz^+\;2C^i(p,k)\left\{1+\frac{i}{2}p^2\frac{z^+}{p^+}-\frac{1}{8}\left(p^2\frac{z^+}{p^+}\right)^2\right\}\rho_T^c(z^+,p-k)\;. \tag{A11}$$

One can now read off the Lipatov vertex at NNE accuracy as written in eq. (6). The first term in the curly brackets corresponds to a straight line trajectory. The second and third terms account for corrections, at $\mathcal{O}(\ell^+)$ and $\mathcal{O}(\ell^{+2})$, respectively, due to quantum diffusion from that classical path. The structure of the vertex in eq. (A11) suggests that the corrections to the amplitude due to a finite target thickness may exponentiate to a phase,

$$\left\{1+\frac{i}{2}p^2\frac{z^+}{p^+}-\frac{1}{8}\left(p^2\frac{z^+}{p^+}\right)^2\right\}\to\exp\left(\frac{i}{2}p^2\frac{z^+}{p^+}\right)\;. \tag{A12}$$

However, a strict proof of exponentiation would require a generalization of eq. (A1) to all orders in ℓ^+/p^+.

Appendix B: Single inclusive gluon production at NNE accuracy

The single inclusive gluon production cross section is given by

$$f^{abc}f^{ab'c'}g^6\int\frac{d^2k_1}{(2\pi)^2}\frac{d^2k_2}{(2\pi)^2}\int dz_1^-dz_2^+d\bar{z}_1^-d\bar{z}_2^+\frac{L_i(p,k_1)L_i^*(p,k_2)}{k_1^2k_2^2(p-k_1)^2(p-k_2)^2} \times\left\langle\rho^b(z_1^-,k_1)\,\rho^{*b'}(\bar{z}_1^-,k_2)\right\rangle_P\left\langle\rho^c(z_2^+,p-k_1)\,\rho^{*c'}(\bar{z}_2^+,p-k_2)\right\rangle_T\;. \tag{B1}$$

With the (re-exponentiated) Lipatov vertex from above and the color charge correlator from eq. (12) this becomes

$$4N_c(N_c^2-1)\,g^4S_\perp\int\frac{d^2k}{(2\pi)^2}\frac{g^2\int dz_1^-\mu_P^2}{k^2}\;\frac{k^2}{(p-k)^4}\mu_T^2\;C^i(p,k)C^i(p,k) \times\int\frac{dz_2^+d\bar{z}_2^+}{2\lambda^+}\,\Theta(\lambda^+-|z_2^+-\bar{z}_2^+|)\,e^{ip^2(z_2^+-\bar{z}_2^+)/2p^+} \tag{B2}$$

$$=\;4N_c(N_c^2-1)\,g^2\frac{S_\perp}{p^2}\frac{2p^+}{p^2\,\lambda^+}\sin\left(\frac{p^2\,\lambda^+}{2p^+}\right)\int\frac{d^2k}{(2\pi)^2}\Phi_P(k^2)\frac{g^2\ell^+\,\mu_T^2}{(p-k)^2}\;. \tag{B3}$$

We have assumed that $\lambda^+\ll\ell^+$. Substituting the unintegrated gluon distribution of the target introduced in eq. (14) and expanding to second order in λ^+ finally leads to

$$4N_c(N_c^2-1)\,g^2\frac{S_\perp}{p^2}\left[1-\frac{1}{6}\left(\frac{p^2\,\lambda^+}{2p^+}\right)^2\right]\int\frac{d^2k}{(2\pi)^2}\Phi_P(k^2)\,\Phi_T((p-k)^2)\;. \tag{B4}$$

Appendix C: Double inclusive gluon production at NNE accuracy

The inclusive two gluon production cross section is given by

$$p^+q^+\frac{d\sigma}{dp^+d^2pdq^+d^2q} = f^{abc}f^{\bar{a}\bar{b}\bar{c}}f^{\bar{a}\bar{b}'\bar{c}'}f^{ab'c'}g^{12}\int\frac{d^2k_1}{(2\pi)^2}\frac{d^2k_2}{(2\pi)^2}\frac{d^2k_3}{(2\pi)^2}\frac{d^2k_4}{(2\pi)^2}\int dz_1^-d\bar{z}_1^-d\omega_1^-d\bar{\omega}_1^-dz_2^+d\bar{z}_2^+d\omega_2^+d\bar{\omega}_2^+$$
$$\times\frac{L^i(p,k_1;z_2^+)}{k_1^2(p-k_1)^2}\frac{L^{*i}(p,k_4;\bar{z}_2^+)}{k_4^2(p-k_4)^2}\frac{L^j(q,k_2;\omega_2^+)}{k_2^2(q-k_2)^2}\frac{L^{*j}(q,k_3;\bar{\omega}_2^+)}{k_3^2(q-k_3)^2}\left\langle\rho^b(z_1^-,k_1)\rho^{\bar{b}}(\omega_1^-,k_2)\rho^{*\bar{b}'}(\bar{\omega}_1^-,k_3)\rho^{*b'}(\bar{z}_1^-,k_4)\right\rangle_P$$
$$\times\left\langle\rho^c(z_2^+,p-k_1)\rho^{\bar{c}}(\omega_2^+,q-k_2)\rho^{*\bar{c}'}(\bar{\omega}_2^+,q-k_3)\rho^{*c'}(\bar{z}_2^+,p-k_4)\right\rangle_T \tag{C1}$$

We shall use the local correlator of color charges as written in eq. (10).

Type A contributions correspond to the following contraction on the target side:

$$\left\langle\rho^c(z_2^+,p-k_1)\rho^{\bar{c}}(\omega_2^+,q-k_2)\rho^{*\bar{c}'}(\bar{\omega}_2^+,q-k_3)\rho^{*c'}(\bar{z}_2^+,p-k_4)\right\rangle_T \to \left\langle\rho^c(z_2^+,p-k_1)\rho^{*c'}(\bar{z}_2^+,p-k_4)\right\rangle_T$$
$$\times\left\langle\rho^{\bar{c}}(\omega_2^+,q-k_2)\rho^{*\bar{c}'}(\bar{\omega}_2^+,q-k_3)\right\rangle_T . \tag{C2}$$

Using eq. (10) it is straightforward to see that Type A contributions to the cross section are proportional to

$$(2\pi)^4\delta^{cc'}\delta^{\bar{c}\bar{c}'}\delta(z_2^+-\bar{z}_2^+)\delta(\omega_2^+-\bar{\omega}_2^+)\delta^{(2)}(k_1-k_4)\delta^{(2)}(k_2-k_3)\mu_T^2(z_2{}^+)\mu_T^2(\omega_2^+) . \tag{C3}$$

However, realizing the longitudinal δ-functions in eq. (C3), one can easily see that sub-eikonal corrections to the Type A contributions for the double inclusive gluon production cross section vanish.

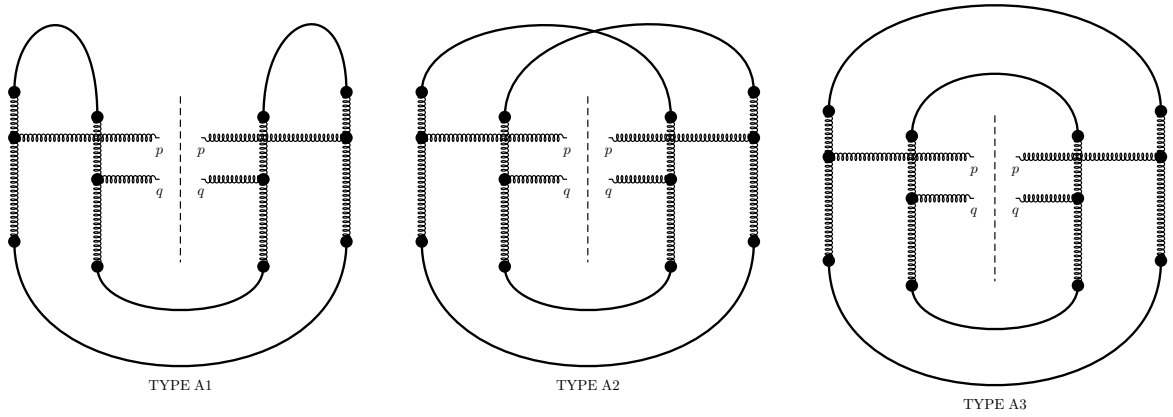

FIG. 3: Type A contributions to the double inclusive gluon production

After performing the color contractions on the projectile side we get three types of diagrams: Type A1, Type A2 and Type A3 (see Fig. 3):

$$\text{Type A1} \propto (2\pi)^2\delta^{b\bar{b}}\delta^{\bar{b}'b'}\delta(z_1^- - \omega_1^-)\delta(\bar{z}_1^- - \bar{\omega}_1^-)\delta^{(2)}(k_1+k_2)\delta^{(2)}(k_3+k_4)\mu_P^2(z_1^-)\mu_P^2(\bar{z}_1^-) \tag{C4}$$
$$\text{Type A2} \propto (2\pi)^2\delta^{b\bar{b}'}\delta^{\bar{b}b'}\delta(z_1^- - \bar{\omega}_1^-)\delta(\bar{z}_1^- - \omega_1^-)\delta^{(2)}(k_1-k_3)\delta^{(2)}(k_2-k_4)\mu_P^2(z_1^-)\mu_P^2(\bar{z}_1^-) \tag{C5}$$
$$\text{Type A3} \propto (2\pi)^2\delta^{bb'}\delta^{\bar{b}\bar{b}'}\delta(z_1^- - \bar{z}_1^-)\delta(\omega_1^- - \bar{\omega}_1^-)\delta^{(2)}(k_1-k_4)\delta^{(2)}(k_2-k_3)\mu_P^2(z_1^-)\mu_P^2(\bar{\omega}_1^-) . \tag{C6}$$

Using eqs. (C3 - C6) these contributions become

$$\text{Type A1} = f^{abc} f^{\bar{a}b\bar{c}} f^{\bar{a}\bar{b}\bar{c}} f^{a\bar{b}c} S_\perp g^8 \int \frac{d^2k_1}{(2\pi)^2}\frac{d^2k_3}{(2\pi)^2}\delta^{(2)}(k_1+k_3)\Phi_P(k_1^2)\Phi_P(k_3^2)\int dz_2^+ d\omega_2^+ \mu_T^2(z_2^+)\mu_T^2(\omega_2^+)$$
$$2^4 C^i(p,k_1)C^i(p,-k_3)C^j(q,-k_1)C^j(q,k_3)\frac{k_1^2 k_3^2}{(p-k_1)^2(p+k_3)^2(q+k_1)^2(q-k_3)^2} \tag{C7}$$

$$\text{Type A2} = f^{abc} f^{\bar{a}\bar{b}\bar{c}} f^{\bar{a}b\bar{c}} f^{a\bar{b}c} S_\perp g^8 \int \frac{d^2k_1}{(2\pi)^2}\frac{d^2k_2}{(2\pi)^2}\delta^{(2)}(k_1-k_2)\Phi_P(k_1^2)\Phi_P(k_2^2)\int dz_2^+ d\omega_2^+ \mu_T^2(z_2^+)\mu_T^2(\omega_2^+)$$
$$2^4 C^i(p,k_1)C^i(p,k_1)C^j(q,k_2)C^j(q,k_2)\frac{k_1^2 k_2^2}{(p-k_1)^4(q-k_2)^4} \tag{C8}$$

$$\text{Type A3} = f^{abc} f^{\bar{a}\bar{b}\bar{c}} f^{\bar{a}\bar{b}\bar{c}} f^{abc} S_\perp^2 g^8 \int \frac{d^2k_1}{(2\pi)^2}\frac{d^2k_2}{(2\pi)^2}\Phi_P(k_1^2)\Phi_P(k_2^2)\int dz_2^+ d\omega_2^+ \mu_T^2(z_2^+)\mu_T^2(\omega_2^+)$$
$$2^4 C^i(p,k_1)C^i(p,k_1)C^j(q,k_2)C^j(q,k_2)\frac{k_1^2 k_2^2}{(p-k_1)^4(q-k_2)^4} \tag{C9}$$

Note that we have used eq. (14) to define the unintegrated gluon distribution of the projectile and eq. (6) for the definition of the Lipatov vertex at NNE accuracy. To simplify the expressions further we integrate over the longitudinal coordinate and substitute the unintegrated gluon distribution of the target:

$$\text{Type A1} = 16N_c^2(N_c^2-1)\,g^4\frac{S_\perp}{p^2q^2}\int\frac{d^2k_1}{(2\pi)^2}\frac{d^2k_2}{(2\pi)^2}\delta^{(2)}(k_1+k_2)\Phi_P(k_1^2)\Phi_T\left[(p-k_1)^2\right]\Phi_P(k_2^2)\Phi_T\left[(q-k_2)^2\right] \tag{C10}$$

$$\text{Type A2} = 16N_c^2(N_c^2-1)\,g^4\frac{S_\perp}{p^2q^2}\int\frac{d^2k_1}{(2\pi)^2}\frac{d^2k_2}{(2\pi)^2}\delta^{(2)}(k_1-k_2)\Phi_P(k_1^2)\Phi_T\left[(p-k_1)^2\right]\Phi_P(k_2^2)\Phi_T\left[(q-k_2)^2\right] \tag{C11}$$

$$\text{Type A3} = 16N_c^2(N_c^2-1)^2\,g^4\frac{S_\perp^2}{p^2q^2}\int\frac{d^2k_1}{(2\pi)^2}\frac{d^2k_2}{(2\pi)^2}\Phi_P(k_1^2)\Phi_T\left[(p-k_1)^2\right]\Phi_P(k_2^2)\Phi_T\left[(q-k_2)^2\right]\,. \tag{C12}$$

As already mentioned above subeikonal corrections vanish for these diagrams. The last expression, eq. (C12), is of course nothing but the uncorrelated square of the single inclusive cross section.

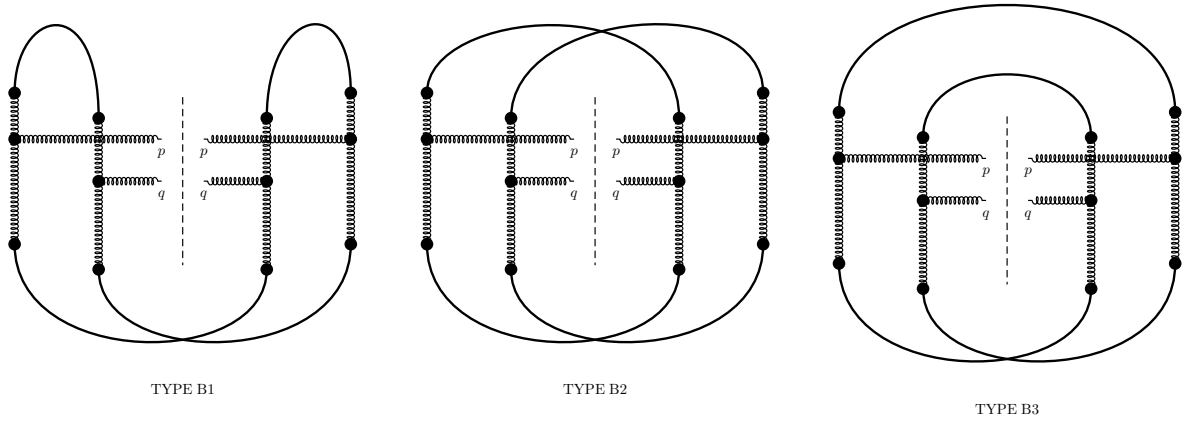

FIG. 4: Type B contributions to the double inclusive gluon production

Type B contributions correspond to the following color contraction on the target side:

$$\left\langle \rho^c(z_2^+,p-k_1)\rho^{\bar{c}}(\omega_2^+,q-k_2)\rho^{*\bar{c}'}(\bar{\omega}_2^+,q-k_3)\rho^{*c'}(\bar{z}_2^+,p-k_4)\right\rangle_T \;\to\; \left\langle \rho^c(z_2^+,p-k_1)\rho^{*\bar{c}'}(\bar{\omega}_2^+,q-k_3)\right\rangle_T$$
$$\times\left\langle \rho^{\bar{c}}(\omega_2^+,q-k_2)\rho^{*c'}(\bar{z}_2^+,p-k_4)\right\rangle_T\,. \tag{C13}$$

Again, by using eq. (10), one finds that Type B contributions are proportional to

$$(2\pi)^4\delta^{c\bar{c}'}\delta^{\bar{c}c'}\delta(z_2^+-\bar{\omega}_2^+)\delta(\omega_2^+-\bar{z}_2^+)\delta^{(2)}(p-q+k_3-k_1)\delta^{(2)}(q-p+k_4-k_2)\mu_T^2(z_2^+)\mu_T^2(\omega_2^+)\,. \tag{C14}$$

The color contractions on the projectile side are the same as Type A diagrams. Hence, one can immediately write the Type B contributions to the double inclusive gluon production cross section as

$$\text{Type B1} \;=\; f^{abc}f^{\bar{a}\bar{b}\bar{c}}f^{\bar{a}\bar{b}c}f^{a\bar{b}\bar{c}}S_\perp g^8\int\frac{d^2k_1}{(2\pi)^2}\frac{d^2k_3}{(2\pi)^2}\delta^{(2)}(p-q-k_1+k_3)\Phi_P(k_1^2)\Phi_P(k_3^2)\int dz_2^+d\bar{z}_2^+\mu_T^2(z_2^+)\mu_T^2(\bar{z}_2^+)2^4$$
$$C^i(p,k_1)C^i(p,-k_3)C^j(q,-k_1)C^j(q,k_3)\frac{k_1^2k_3^2}{(p-k_1)^2(p+k_3)^2(q+k_1)^2(q-k_3)^2}\left\{1-\frac{1}{8}\left(\frac{p^2}{p^+}-\frac{q^2}{q^+}\right)^2(z_2^+-\bar{z}_2^+)^2\right\}$$
$$=\; 2N_c^2(N_c^2-1)g^4\frac{S_\perp}{p^2q^2}\int\frac{d^2k_1}{(2\pi)^2}\frac{d^2k_2}{(2\pi)^2}\delta^{(2)}(p-q-k_1+k_2)\Phi_P(k_1^2)\Phi_T\left[(p-k_1)^2\right]\Phi_P(k_2^2)\Phi_T\left[(q-k_2)^2\right]$$
$$\times\left\{1+\frac{k_2^2(p-k_1)^2}{k_1^2(p+k_2)^2}-\frac{p^2(k_1+k_2)^2}{k_1^2(p+k_2)^2}\right\}\left\{1+\frac{k_1^2(q-k_2)^2}{k_2^2(q+k_1)^2}-\frac{q^2(k_1+k_2)^2}{k_2^2(q+k_1)^2}\right\}\left[1-\frac{1}{12}\left(\frac{p^2}{2p^+}-\frac{q^2}{2q^+}\right)^2\ell^{+2}\right] \tag{C15}$$

$$\text{Type B2} \;=\; f^{abc}f^{\bar{a}\bar{b}\bar{c}}f^{\bar{a}bc}f^{a\bar{b}\bar{c}}S_\perp g^8\delta^{(2)}(p-q)\int\frac{d^2k_1}{(2\pi)^2}\frac{d^2k_2}{(2\pi)^2}\Phi_P(k_1^2)\Phi_P(k_2^2)\int dz_2^+d\bar{z}_2^+\mu_T^2(z_2^+)\mu_T^2(\bar{z}_2^+)2^4$$
$$C^i(p,k_1)C^i(p,k_2)C^j(q,k_1)C^j(q,k_2)\frac{k_1^2k_2^2}{(p-k_1)^2(p-k_2)^2(q-k_1)^2(q-k_2)^2}\left\{1-\frac{1}{8}\left(\frac{p^2}{p^+}-\frac{q^2}{q^+}\right)^2(z_2^+-\bar{z}_2^+)^2\right\}$$
$$=\; 4N_c^2(N_c^2-1)g^4\frac{S_\perp}{p^2q^2}\delta^{(2)}(p-q)\int\frac{d^2k_1}{(2\pi)^2}\frac{d^2k_2}{(2\pi)^2}\Phi_P(k_1^2)\Phi_T\left[(p-k_1)^2\right]\Phi_P(k_2^2)\Phi_T\left[(q-k_2)^2\right]$$
$$\times\left\{1+\frac{k_2^2(p-k_1)^2}{k_1^2(p-k_2)^2}-\frac{p^2(k_1-k_2)^2}{k_1^2(p-k_2)^2}\right\}\left\{1+\frac{k_1^2(q-k_2)^2}{k_2^2(q-k_1)^2}-\frac{q^2(k_1-k_2)^2}{k_2^2(q-k_1)^2}\right\}\left[1-\frac{1}{12}\left(\frac{p^2}{2p^+}-\frac{q^2}{2q^+}\right)^2\ell^{+2}\right] \tag{C16}$$

$$\text{Type B3} \;=\; f^{abc}f^{\bar{a}\bar{b}\bar{c}}f^{\bar{a}\bar{b}c}f^{ab\bar{c}}S_\perp g^8\int\frac{d^2k_1}{(2\pi)^2}\frac{d^2k_2}{(2\pi)^2}\delta^{(2)}(p-q-k_1+k_2)\Phi_P(k_1^2)\Phi_P(k_2^2)\int dz_2^+d\bar{z}_2^+\mu_T^2(z_2^+)\mu_T^2(\bar{z}_2^+)2^4$$
$$C^i(p,k_1)C^i(p,k_1)C^j(q,k_2)C^j(q,k_2)\frac{k_1^2k_2^2}{(p-k_1)^4(q-k_2)^4}\left\{1-\frac{1}{8}\left(\frac{p^2}{p^+}-\frac{q^2}{q^+}\right)^2(z_2^+-\bar{z}_2^+)^2\right\}$$
$$=\; 16N_c^2(N_c^2-1)g^4\frac{S_\perp}{p^2q^2}\int\frac{d^2k_1}{(2\pi)^2}\frac{d^2k_2}{(2\pi)^2}\delta^{(2)}(p-q-k_1+k_2)\Phi_P(k_1^2)\Phi_T\left[(p-k_1)^2\right]\Phi_P(k_2^2)\Phi_T\left[(q-k_2)^2\right]$$
$$\times\left[1-\frac{1}{12}\left(\frac{p^2}{2p^+}-\frac{q^2}{2q^+}\right)^2\ell^{+2}\right] \tag{C17}$$

To perform the longitudinal integrations explicitly we have assumed that μ_T^2 is constant. Note that for the Type B contributions, next to eikonal contributions to the cross section vanish due to integration over z_2^+ and $\bar{z}_2^+$. However, the next to next to eikonal corrections to the cross sections do not vanish. For Type B1 and Type B2 contributions we have used

$$C^i(p,k_1)C^i(p,k_2)\;=\;\left(\frac{p^i}{p^2}-\frac{k_1^i}{k_1^2}\right)\left(\frac{p^i}{p^2}-\frac{k_2^i}{k_2^2}\right)=\frac{1}{2p^2k_1^2k_2^2}\left[k_1^2(p-k_2)^2+k_2^2(p-k_1)^2-p^2(k_1-k_2)^2\right] \tag{C18}$$

The color contractions on the target side for Type C contributions are given by

$$\left\langle\rho^c(z_2^+,p-k_1)\rho^{\bar{c}}(\omega_2^+,q-k_2)\rho^{*\bar{c}'}(\bar{\omega}_2^+,q-k_3)\rho^{*c'}(\bar{z}_2^+,p-k_4)\right\rangle_T\;\to\;\left\langle\rho^c(z_2^+,p-k_1)\rho^{*\bar{c}}(\omega_2^+,q-k_2)\right\rangle_T$$
$$\times\left\langle\rho^{\bar{c}'}(\bar{\omega}_2^+,q-k_3)\rho^{*c'}(\bar{z}_2^+,p-k_4)\right\rangle_T\;. \tag{C19}$$

Thus, they are proportional to

$$(2\pi)^4\delta^{c\bar{c}}\delta^{\bar{c}'c'}\delta(z_2^+-\omega_2^+)\delta(\bar{z}_2^+-\bar{\omega}_2^+)\delta^{(2)}(p+q-k_1-k_2)\delta^{(2)}(p+q-k_3-k_4)\mu_T^2(z_2^+)\mu_T^2(\bar{z}_2^+)\;. \tag{C20}$$

Since the color contractions on the projectile side are the same as Type A and Type B diagrams, one can write the

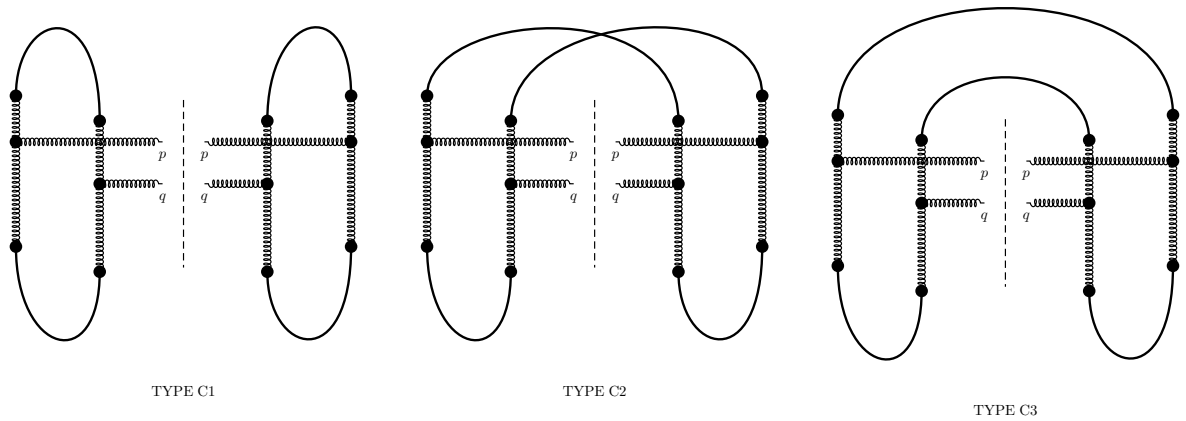

FIG. 5: Type C contributions to the double inclusive gluon production

Type C contributions to the double inclusive gluon production cross section as follows:

$$\begin{aligned}
\text{Type C1} &= f^{abc}f^{\bar{a}bc}f^{\bar{a}\bar{b}\bar{c}}f^{a\bar{b}\bar{c}}S_\perp g^8\delta^{(2)}(p+q)\int\frac{d^2k_1}{(2\pi)^2}\frac{d^2k_3}{(2\pi)^2}\Phi_P(k_1^2)\Phi_P(k_3^2)\int dz_2^+ d\bar{z}_2^+\mu_T^2(z_2^+)\mu_T^2(\bar{z}_2^+)2^4 \\
&\quad C^i(p,k_1)C^i(p,-k_3)C^j(q,-k_1)C^j(q,k_3)\frac{k_1^2k_3^2}{(p-k_1)^2(p+k_3)^2(q+k_1)^2(q-k_3)^2}\left\{1-\frac{1}{8}\left(\frac{p^2}{p^+}+\frac{q^2}{q^+}\right)^2(z_2^+-\bar{z}_2^+)^2\right\} \\
&= 4N_c^2(N_c^2-1)g^4\frac{S_\perp}{p^2q^2}\delta^{(2)}(p+q)\int\frac{d^2k_1}{(2\pi)^2}\frac{d^2k_2}{(2\pi)^2}\Phi_P(k_1^2)\Phi_T\left[(p-k_1)^2\right]\Phi_P(k_2^2)\Phi_T\left[(q-k_2)^2\right] \\
&\times\left\{1+\frac{k_2^2(p-k_1)^2}{k_1^2(p+k_2)^2}-\frac{p^2(k_1+k_2)^2}{k_1^2(p+k_2)^2}\right\}\left\{1+\frac{k_1^2(q-k_2)^2}{k_2^2(q+k_1)^2}-\frac{q^2(k_1+k_2)^2}{k_2^2(q+k_1)^2}\right\}\left[1-\frac{1}{12}\left(\frac{p^2}{2p^+}+\frac{q^2}{2q^+}\right)^2\ell^{+2}\right] \qquad \text{(C21)} \\
\text{Type C2} &= f^{abc}f^{\bar{a}\bar{b}c}f^{\bar{a}b\bar{c}}f^{a\bar{b}\bar{c}}S_\perp g^8\int\frac{d^2k_1}{(2\pi)^2}\frac{d^2k_2}{(2\pi)^2}\delta^{(2)}(p+q-k_1-k_2)\Phi_P(k_1^2)\Phi_P(k_2^2)\int dz_2^+ d\bar{z}_2^+\mu_T^2(z_2^+)\mu_T^2(\bar{z}_2^+)2^4 \\
&\quad C^i(p,k_1)C^i(p,k_2)C^j(q,k_1)C^j(q,k_2)\frac{k_1^2k_2^2}{(p-k_1)^2(p-k_2)^2(q-k_1)^2(q-k_2)^2}\left\{1-\frac{1}{8}\left(\frac{p^2}{p^+}+\frac{q^2}{q^+}\right)^2(z_2^+-\bar{z}_2^+)^2\right\} \\
&= 2N_c^2(N_c^2-1)g^4\frac{S_\perp}{p^2q^2}\int\frac{d^2k_1}{(2\pi)^2}\frac{d^2k_2}{(2\pi)^2}\delta^{(2)}(p+q-k_1-k_2)\Phi_P(k_1^2)\Phi_T\left[(p-k_1)^2\right]\Phi_P(k_2^2)\Phi_T\left[(q-k_2)^2\right] \\
&\times\left\{1+\frac{k_2^2(p-k_1)^2}{k_1^2(p-k_2)^2}-\frac{p^2(k_1-k_2)^2}{k_1^2(p-k_2)^2}\right\}\left\{1+\frac{k_1^2(q-k_2)^2}{k_2^2(q-k_1)^2}-\frac{q^2(k_1-k_2)^2}{k_2^2(q-k_1)^2}\right\}\left[1-\frac{1}{12}\left(\frac{p^2}{2p^+}+\frac{q^2}{2q^+}\right)^2\ell^{+2}\right] \qquad \text{(C22)} \\
\text{Type C3} &= f^{abc}f^{\bar{a}\bar{b}c}f^{\bar{a}\bar{b}\bar{c}}f^{ab\bar{c}}S_\perp g^8\int\frac{d^2k_1}{(2\pi)^2}\frac{d^2k_2}{(2\pi)^2}\delta^{(2)}(p+q-k_1-k_2)\Phi_P(k_1^2)\Phi_P(k_2^2)\int dz_2^+ d\bar{z}_2^+\mu_T^2(z_2^+)\mu_T^2(\bar{z}_2^+)2^4 \\
&\quad C^i(p,k_1)C^i(p,k_1)C^j(q,k_2)C^j(q,k_2)\frac{k_1^2k_2^2}{(p-k_1)^4(q-k_2)^4}\left\{1-\frac{1}{8}\left(\frac{p^2}{p^+}+\frac{q^2}{q^+}\right)^2(z_2^+-\bar{z}_2^+)^2\right\} \\
&= 16N_c^2(N_c^2-1)g^4\frac{S_\perp}{p^2q^2}\int\frac{d^2k_1}{(2\pi)^2}\frac{d^2k_2}{(2\pi)^2}\delta^{(2)}(p+q-k_1-k_2)\Phi_P(k_1^2)\Phi_T\left[(p-k_1)^2\right]\Phi_P(k_2^2)\Phi_T\left[(q-k_2)^2\right] \\
&\quad\times\left[1-\frac{1}{12}\left(\frac{p^2}{2p^+}+\frac{q^2}{2q^+}\right)^2\ell^{+2}\right]. \qquad \text{(C23)}
\end{aligned}$$

[1] Yu. V. Kovchegov, E. Levin: "Quantum Chromodynamics at High Energy", Cambridge Monographs, Cambridge Univ. Press (2012)

[2] A. Kovner, L. D. McLerran and H. Weigert, Phys. Rev. D **52**, 6231 (1995); Phys. Rev. D **52**, 3809 (1995).

[3] Yu. V. Kovchegov and D. H. Rischke, Phys. Rev. C **56**, 1084 (1997) [hep-ph/9704201].

[4] J. P. Blaizot, F. Gelis and R. Venugopalan, Nucl. Phys. A **743**, 13 (2004) [hep-ph/0402256].

[5] L. N. Lipatov, Sov. J. Nucl. Phys. **23**, 338 (1976) [Yad. Fiz. **23**, 642 (1976)]; E. A. Kuraev, L. N. Lipatov and V. S. Fadin, Sov. Phys. JETP **45**, 199 (1977) [Zh. Eksp. Teor. Fiz. **72**, 377 (1977)]; I. I. Balitsky and L. N. Lipatov, Sov. J. Nucl. Phys. **28**, 822 (1978) [Yad. Fiz. **28**, 1597 (1978)].

[6] A. Dumitru and L. D. McLerran, Nucl. Phys. A **700**, 492 (2002) [hep-ph/0105268].

[7] I. Balitsky and A. Tarasov, JHEP **1510**, 017 (2015) [arXiv:1505.02151 [hep-ph]].

[8] A. Babansky and I. Balitsky, Phys. Rev. D **67**, 054026 (2003).

[9] T. Altinoluk, N. Armesto, G. Beuf, M. Martinez and C. A. Salgado, JHEP **1407**, 068 (2014) [arXiv:1404.2219 [hep-ph]].

[10] T. Altinoluk, N. Armesto, G. Beuf and A. Moscoso, JHEP **1601**, 114 (2016) [arXiv:1505.01400 [hep-ph]].

[11] L. D. McLerran and R. Venugopalan, Phys. Rev. **D 49**, 2233 (1994), Phys. Rev. **D 49**, 3352 (1994); Yu. V. Kovchegov, Phys. Rev. **D 54**, 5463 (1996).

[12] A. Dumitru, F. Gelis, L. McLerran and R. Venugopalan, Nucl. Phys. A **810**, 91 (2008) [arXiv:0804.3858 [hep-ph]]; A. Dumitru, K. Dusling, F. Gelis, J. Jalilian-Marian, T. Lappi and R. Venugopalan, Phys. Lett. B **697**, 21 (2011) [arXiv:1009.5295 [hep-ph]].

[13] The eikonal case has been studied in detail by K. Dusling and R. Venugopalan, Phys. Rev. D **87**, no. 5, 051502 (2013) [arXiv:1210.3890 [hep-ph]]; Phys. Rev. D **87**, no. 5, 054014 (2013) [arXiv:1211.3701 [hep-ph]].

[14] The most direct way to see this is to note that the correction in curly brackets in eq. (6) corresponds to the first three terms in the Taylor series expansion of the phase $\exp\left(\frac{i}{2}p^2\frac{z_2^+}{p^+}\right)$.

[15] To obtain the field analogous to eq. (1) one would strip off the polarization vector, multiply by the projectile charge density $g\rho_P(z_1^-,k)$, and integrate over dz_1^- and $d^2k/(2\pi)^2$.

[16] The expression written in ref. [10] is missing a factor of 1/2 in the term $\sim \mathcal{U}^{jl}_{[0,2]}(\ell^+,0;x)$ which we have corrected.